Combination Neoantigen-Based Dendritic Cell Vaccination and Adoptive T-Cell Transfer Induces Antitumor Responses Against Recurrence of Hepatocellular Carcinoma

Sui Peng[1,2], Shuling Chen[3], Wei Hu[1], Jie Mei[2], Xuezhen Zeng[1,4], Tianhong Su[5], Wei Wang[3], Zebin Chen[6], Han Xiao[3], Qian Zhou[2], Bin Li[2], Yubin Xie[1], Huanjing Hu[1], Minghui He[1], Yanyan Han[7], Longqing Tang[7], Yifan Ma[7], Xiaoshuang Li[7], Xiangjun Zhou[7], Zihao Dai[6], Zelong Liu[3], Jiehui Tan[8], Lixia Xu[5], Shaoqiang Li[6], Shunli Shen[6], Dongming Li[6], Jiaming Lai[9], Baogang Peng[6], Zhenwei Peng[10,11], and Ming Kuang[6]

ABSTRACT

A high rate of recurrence after curative therapy is a major challenge for the management of hepatocellular carcinoma (HCC). Currently, no effective adjuvant therapy is available to prevent HCC recurrence. We designed a personalized neoantigen-loaded dendritic cell vaccine and neoantigen-activated T-cell therapy, and used it as adjuvant therapy to treat 10 patients with HCC who had undergone curative resection or radiofrequency ablation in the first stage of a phase II trial (NCT03067493). The primary outcomes were safety and neoantigen-specific immune response. Disease-free survival (DFS) was also evaluated. The immunotherapy was successfully administered to all the patients without unexpected delay and demonstrated a reasonable safety profile with no grade ≥3 treatment-related side effects reported. Seventy percent of patients generated *de novo* circulating multiclonal neoantigen-specific T-cell responses. Induced neoantigen-specific immunity was maintained over time, and epitope spreading was observed. Patients who generated immune responses to treatment exhibited prolonged DFS compared with nonresponders ($P = 0.012$), with 71.4% experiencing no relapse for 2 years after curative treatment. High expression of an immune stimulatory signature, enhanced immune-cell infiltration (i.e., $CD8^+$ T cells), and upregulated expression of T-cell inflammatory gene profiles were found in the primary tumors of the responders. In addition, neoantigen depletion (immunoediting) was present in the recurrent tumors compared with the primary tumors (7/9 vs. 1/17, $P = 0.014$), suggesting that immune evasion occurred under the pressure of immunotherapy. Our study indicates that neoantigen-based combination immunotherapy is feasible, safe, and has the potential to reduce HCC recurrence after curative treatment.

Introduction

Approximately 70% of hepatocellular carcinoma (HCC) cases recur within 5 years of curative treatment (1). The high rate of recurrence highlights the urgent need for adjuvant therapies (2). Many therapies, like transarterial chemoembolization (TACE) and chemotherapy, have been used to prevent HCC recurrence, but it remains unclear how beneficial these are (3–5). The international "STORM" trial investigated the use of sorafenib versus placebo as an adjuvant therapy to reduce HCC recurrence, but no benefit was observed (6). The failure of the STORM trial may be partly due to the substantial heterogeneity among HCC tumors and patients (7, 8). Therefore, development of new, effective, personalized adjuvant treatments for the prevention of HCC recurrence is urgently needed.

Immune checkpoint inhibitors have achieved promising results for many types of cancer (9–12). However, the objective response rate is only around 20% in patients with advanced HCC (9, 13). Therefore, there has been a great deal of interest in designing a personalized strategy to improve immunotherapy efficacy (14). Neoantigens are mutated antigens specifically expressed by cancer cells with high individual specificity and can induce robust specific antitumor immunity (15, 16). Effective antitumor immunity is strongly associated with the presence of T cells directed at tumor-specific antigens (15);

[1]Institute of Precision Medicine, The First Affiliated Hospital, Sun Yat-sen University, Guangzhou, Guangdong, China. [2]Clinical Trials Unit, The First Affiliated Hospital, Sun Yat-sen University, Guangzhou, Guangdong, China. [3]Division of Interventional Ultrasound, The First Affiliated Hospital, Sun Yat-sen University, Guangzhou, Guangdong, China. [4]Department of Pharmacy, The First Affiliated Hospital, Sun Yat-sen University, Guangzhou, Guangdong, China. [5]Department of Medical Oncology, The First Affiliated Hospital, Sun Yat-sen University, Guangzhou, Guangdong, China. [6]Department of Liver Surgery, Center of Hepato-Pancreato-Biliary Surgery, The First Affiliated Hospital, Sun Yat-sen University, Guangzhou, Guangdong, China. [7]HRYZ Biotech Co., Shenzhen, China. [8]Organ Transplant Center, The First Affiliated Hospital, Sun Yat-sen University, Guangzhou, Guangdong, China. [9]Department of Pancreaticobiliary Surgery, Center of Hepato-Pancreato-Biliary Surgery, The First Affiliated Hospital, Sun Yat-sen University, Guangzhou, Guangdong, China. [10]Cancer Center, The First Affiliated Hospital of Sun Yat-sen University, Guangzhou, Guangdong, China. [11]Department of Radiation Oncology, The First Affiliated Hospital of Sun Yat-sen University, Guangzhou, Guangdong, China.

Note: Supplementary data for this article are available at Cancer Immunology Research Online (http://cancerimmunolres.aacrjournals.org/).

S. Peng, S. Chen, W. Hu, J. Mei, and X. Zeng contributed equally to this article.

Corresponding Authors: Ming Kuang, No. 58, Zhongshan Er Road, The First Affiliated Hospital of Sun Yat-sen University, Guangzhou 510080, Guangdong Province, P.R. China. Phone: 8620-8775-5766, ext. 8214; Fax: 8620-8776-6335; E-mail: kuangm@mail.sysu.edu.cn; and Zhenwei Peng, pzhenw@mail.sysu.edu.cn

Cancer Immunol Res 2022;10:728–44

doi: 10.1158/2326-6066.CIR-21-0931

therefore, increasing the presentation of neoantigens and the quantity of neoantigen-specific T cells is critical. Adoptive cellular therapy (ACT) can actively increase a patient's T-cell numbers (17, 18). Currently, however, these adoptive T-cell therapies are mainly specific for tumor-associated antigens (TAA), rather than neoantigens, and therefore they are not tumor-specific, leading to problems of insufficient antitumor effects (19). In recent years, neoantigen vaccines in the form of dendritic cells (DC), peptides, or mRNAs have been demonstrated to be feasible, safe, and capable of inducing specific antitumor immune responses in melanoma and glioblastoma (20–24). In addition, neoantigen-specific T-cell receptor (TCR)-expressing T cells have been designed and shown to successfully eliminate large solid tumors in mice (25). However, the clinical efficacy of neoantigen vaccines and TCR-based ACT monotherapies in patients with solid tumors remain to be proven (26).

Combination therapy is currently a major trend in cancer immunotherapy. A neoantigen-loaded DC vaccine has the potential to induce long-term immunity by increasing neoantigen presentation, activating host antigen-specific T cells, and accelerating T-cell homing (14, 21, 27), but its efficacy as a monotherapy might be restricted due to potential issues of the immunosuppressive microenvironment and T-cell dysfunction (22, 28). Given that neoantigen-activated T-cell therapy has the potential to boost the quantity of tumor-specific T cells in a short period of time, we hypothesized that combining these two neoantigen-based immunotherapy approaches could augment the rate and durability of the antitumor immune response and eventually result in an improved clinical outcome. To the best of our knowledge, no previous study has ever evaluated the potential of this combination neoantigen-based immunotherapy against cancer.

In this study, we report the results of the first stage of the ongoing RAMEC trial (NCT03067493) to investigate the safety, efficacy and immunologic effects of combination treatment with a neoantigen-loaded DC vaccine and neoantigen-activated T-cell therapy to prevent HCC recurrence after surgical resection or radiofrequency ablation (RFA). In addition, we also performed comprehensive bioinformatic and immune analyses to explore the factors associated with the immune response and recurrence using serial tumor tissue samples and peripheral blood mononuclear cells (PBMC) obtained prior to curative treatment, before immunotherapy, and after immunotherapy.

Materials and Methods

Study design

This is the first stage of an open-label phase II clinical trial (NCT03067493) where the safety and immunologic effect of adjuvant neoantigen-based combination immunotherapy after resection or RFA for patients with HCC is evaluated. We recruited 10 patients for safety evaluation and immune response assessment. The study design is shown in Supplementary Fig. S1. In brief, the design was that 3 patients would be recruited and safety assessed after one cycle of combined immunotherapy; if no dose-limiting toxicity (DLT) occurred, another 7 patients would be recruited; if 2 or more patients developed DLT, the study would be terminated; if only 1 patient developed DLT, then the procedure would be repeated until 10 patients were recruited; only if the immune response rate was over 50% could the second stage of the trial be started (a phase II randomized clinical trial).

Patients were enrolled based on eligibility assessments at two time points, before resection/RFA and 4 weeks after resection/RFA (**Fig. 1A**). The key inclusion criteria before resection/RFA were: age ≥ 18 years; primary patient with HCC receiving RFA or resection as initial treatment; a solitary tumor measuring 2.0 to 5.0 cm in diameter or 2 to 3 tumors with the largest ≤ 5.0 cm; without vascular invasion, lymphatic metastasis, or distant metastasis; Eastern Cooperative Oncology Group (ECOG) score of 0/1; Child–Pugh score 5 to 7; life expectancy of 6 months or more; adequate hematologic, liver, and renal function. The main inclusion criteria at 4 weeks after resection/RFA were: curative resection or ablation confirmed by contrast-enhanced CT/MRI; successful harvesting of adequate samples of matched tumor and adjacent nontumor normal liver tissues; sensitive mutations detected by gene sequencing in tumor tissue; prediction of ≥10 neoantigen peptides; successful synthesis of ≥5 neoantigen peptides. Other detailed inclusion and exclusion criteria are described in the online Supplementary Methods. Only patients who fulfilled all of these eligibility criteria were enrolled.

In this trial, resection or RFA were performed, and matched tumor and adjacent normal nontumor liver tissue samples were obtained during the treatments. The patients decided between resection and RFA after detailed counselling for the pros and cons of both treatments by attending physicians. Whole-exome sequencing (WES) and RNA sequencing (RNA-seq) were performed to identify tumor-specific mutations, and this information was used to predict neoantigens that would likely be processed and bound to autologous human leukocyte antigen (HLA) class I alleles. For epitope prediction, we adopted two independent methods and selected the top-ranked epitopes from both methods to select neoantigen peptides for therapy (see Prediction of personalized neoantigens). Contrast-enhanced CT/MRI was performed 4 weeks after resection/RFA to evaluate whether curative resection or ablation had been achieved. For the enrolled patients, selected neoantigen peptides were manufactured under GMP conditions. Then, the neoantigen-loaded DC vaccine and neoantigen-activated T cells were prepared and administered to patients following the predefined protocol (**Fig. 1B**). One course of treatment consisted of three cycles of the adjuvant combined immunotherapy. The priming vaccine dose of the DC vaccine was administered in the first cycle, followed by two booster doses for the remaining two cycles in the first course and three booster doses in each following course. DC vaccination followed by adoptive T-cell therapy was administered in one cycle, and repeated throughout the 18 cycles of the adjuvant combination immunotherapy. Since the recurrence rate of HCC in the first year is approximately two times higher than that in the second year (29), the adjuvant combination immunotherapy was administered to patients once a month in the first year and once every second month in the second year. During neoepitope discovery and neoantigen peptide manufacturing (4 months on average), patients received TAA-based immunotherapy until the synthesis of the neoantigen peptides (20, 24). PBMCs were collected via leukapheresis before the beginning of each course of the adjuvant combination immunotherapy for the purpose of preparing the neoantigen-based combination immunotherapy and evaluating the patients' immune responses to neoantigen for each course via ELISPOT assay.

The patients received treatment cycles until unacceptable toxicity, withdrawal of consent, or recurrence. During treatment, the patients had follow-up every 3 months or anytime they felt uncomfortable. After completion of the adjuvant combination immunotherapy, the patients had follow-up every 3 months in the first year and every 4 months thereafter. The trial protocol and all amendments were approved by the trial management team. The trial was conducted following the Declaration of Helsinki and Good Clinical Practice Guidelines and with approval from the institutional ethics committee for Clinical Research and Animal Trials of the First Affiliated Hospital of Sun Yat-sen University (Guangzhou, Guangdong, China). All

patients provided written informed consent both before enrollment and before registration, following the trial protocol. The patients were enrolled from September 25, 2017, to November 26, 2018. The date of the final follow-up was November 26, 2020.

Study end points

The primary outcomes were safety and neoantigen-specific immune response. Safety was evaluated after 9 patients had received at least one cycle of adjuvant combination therapy by recording DLT, which was defined as any grade ≥ 3 hematologic toxicity or nonhematologic toxicity [based on the Common Terminology Criteria for Adverse Event (CTCAE), version 4.0], alopecia not included. In addition, the following events occurring within 7 days after cell injection or infusion were considered to be severe adverse events (AE) grade ≥ 2 uveitis and grade ≥ 2 interstitial pneumonia. The adjuvant combination immunotherapy was considered safe if no DLT occurred. A neoantigen-specific immune response was defined as a positive neoantigen ELISPOT test after the combination immunotherapy. The threshold for a positive response was set at a net 50 spots per 1×10^6 cells, and a positive neoantigen-specific immune response rate over 50% was considered as the success criteria for inducing an immune response. Responders were defined as patients who generated an immune response to the neoantigen-based combination immunotherapy. Disease-free survival (DFS) was also evaluated. It was defined as the time from curative treatment to tumor recurrence, metastasis, or death from any cause, whichever occurred first.

Preclinical safety evaluation

Male and female NOD/SCID mice aged 3 to 4 weeks old were purchased from Beijing Vital River Laboratory Animal Technology Co., Ltd and housed under pathogen-free conditions at the animal facility of Guangdong Lewwin Pharmaceutical Research Institute Co., Ltd. All experiments were performed according to protocols approved by the Institutional Animal Care and Use Committee of Guangdong Lewwin Pharmaceutical Research Institute Co., Ltd (approval number IA-SE2020074–01).

Mice were randomly separated into three groups, A, B, and C, in which mice were given vehicle, low dose of treatment (two times of clinical dose), and high dose of treatment (five times of clinical dose), respectively. LW2011–01 and LW2011–02 are cell products containing T cells and DC, which were generated as described below (see Neoantigen-loaded DC vaccine and neoantigen-activated T-cell preparation). These cell products were given to mice by subcutaneous injection or tail vein injection respectively. Specifically, LW2011–02 was subcutaneously injected on day 1, day 3, and day 5, and then LW2011–01 was injected intravenously via the tail vein on day 8, day 10, and day12. Three days later, one dose of LW2011–02 was administered subcutaneously followed by one intravenous dose of LW2011–01 via tail vein injection 2 days afterwards (as one cycle). Ten more treatment cycles were administered followed by a 42-day recovery period before the mice were sacrificed. Grouping, number of mice, and treatment details are listed in Supplementary Table S1, and the experimental design is summarized in Supplementary Fig. S2.

The preclinical experiment data on safety of DC vaccine and T-cell transfer are reported in Supplementary Tables S1 to S9.

Prediction of personalized neoantigens

The personalized neoantigens were predicted using WES (depth: 352.4×) and RNA-seq data generated from fresh-frozen match tumors and adjacent nontumor liver tissue samples obtained during resection/RFA. Somatic mutations including single-nucleotide variation (SNV) and short insertions and deletions (indels) were filtered with an allele fraction more than 5% and at least 10 supported reads. Subsequently, all mutations were confirmed by RNA-seq data in which there was at least one mutated read. For nonsynonymous mutations, peptide sequences of 31 or 33 amino acids in length were extracted with the mutated site located at the central site for epitope predictions. Neo–open reading frames caused by inframshift mutation were also predicted by extracting several amino acids ahead of mutation sites and extending to the first stop codon. Details of the WES and RNA-seq protocols can be found below (see Exome capture, library preparation, and sequencing and RNA-sequencing data analysis). Patient HLA allotype was assessed with sequencing-based typing using the Sanger method (ABI 3730xl). Each HLA locus was amplified using 200-ng template genomic DNA, amplification primer mix (NGSgo-AmpX), and GenDx-LongRange PCR kit (GenDx). HLA amplicons were verified on an agarose gel and the amplicon concentration was determined by Qubit (Qubit DNA BR Assay Kit, Thermo Fisher Scientific). After quantification, the amplicons of different HLA loci per sample were pooled in equimolar ratios prior to library preparation. The ends of DNA fragment were repaired (NGSgo-LibrX) and Illumina Adaptor was added (NGSgo-IndX). After adapter ligation, the individual libraries were pooled together in equivolume ratio. Size-selection and clean-up of the library pool was performed with solid phase reverse immobilization beads. Finally the libraries were sequenced on Illumina platform (Illumina) with 150 base paired-end reads. The next-generation sequencing (NGS) data were analyzed with the software package NGSengine (GenDx) to determine the HLA genotype.

For epitope prediction, we adopted two methods independently, and selected the top-ranked ones from both methods to get the final peptides for therapy (priority was given to the common peptides predicted by both methods). In the first method, netMHC4.0 and netMHCpan2.8 were used to predict the binding affinity to individual HLA alleles, and netMHCstab1.0 and netMHCstabpan1.0 were used to predict the binding stability (30–32). Epitopes were defined by the stability over 2 hours and higher than that of the corresponding wild type (33). The long peptide neoantigens were ranked in the following order: (i) containing more than two epitopes, (ii) only one high affinity epitope with less than 150 nmol/L, (iii) only one epitope with affinity between 150 and 500 nmol/L, (iv) only one weak epitope more than 500 nmol/L. The ranked neoantigens were then BLAST against the other normal peptides (34), and sequences with 100% identity were discarded. In the second method, all mutations were manually checked by the Integrative Genomics Viewer (IGV) for both WES and RNA-seq data (35). NetMHCpan4.0 was used to predict the binding affinity. The peptides were chosen based on the following criteria: (i) the binding affinity between HLA and mutant peptide was ranked in the top 2%; (ii) the fold change of binding affinity (nM) of mutant/wild-type (WT) was less than 0.5; (iii) the expression level [reads per kilobase per million (RPKM)] of the mutated gene in tumor sample was larger than 1. Finally, up to 11 neoantigen peptides were selected for each patient.

Exome capture, library preparation, and sequencing

Total DNA was extracted from the above tissues using the QIAGEN DNeasy Blood & Tissue Kit (Qiagen, catalog no. 69581). The qualified genomic DNA of tumor and matched adjacent normal tissue from patients with HCC was fragmented to 200 to 300 bp by Covaris technology with resultant library (KAPA Biosystems, catalog no. KK8504; Roche Diagnostics), and then adapters were ligated to both ends of the fragments. Next, extracted DNA was amplified by ligation-mediated PCR (LM-PCR), then purified and hybridized used the xGen

Exome Research Panel v1 (Integrated DNA Technologies, Inc., catalog no. 1056115) for enrichment. Nonhybridized fragments were washed out with xGen Hybridization and Wash kit (Integrated DNA Technologies, Inc., catalog no. 1080584). Each captured library was then loaded on a NovaSeq S4 PE150 instrument (Illumina Inc.) and sequencing was performed using a NovaSeq 6000 S1 Reagent Kit v1.5 (Illumina Inc., catalog no. 20028317). The sequences of each individual were generated as 150-bp paired-end reads.

Reads mapping and variation detection

Raw sequencing reads from the WES were first input to FastQC (https://www.bioinformatics.babraham.ac.uk/projects/fastqc/) to check the sequencing quality, and adapter sequences were trimmed by cutadapt. Then, high quality reads were gapped aligned to the NCBI human reference genome (hg19) (https://hgdownload.cse.ucsc.edu/goldenPath/hg19/bigZips/hg19.fa.gz) using Burrows-Wheeler Aligner (BWA; ref. 36) by default parameters. We performed local realignment of the original BAM alignment using the GATK (37) package and followed by Picard (https://broadinstitute.github.io/picard/) to mark duplicates reads.

Somatic substitutions were detected by MuTect2 (38) based on BWA alignment and only high confident somatic SNVs were retained when the following criteria were met: (i) both the tumor and normal samples were covered sufficiently (≥10×) at the genomic position; (ii) the variants were supported by at least 5% of the total reads in the tumor and less than 1% in the normal; (iii) the variants were supported by at least five reads in the tumor.

High confident somatic indels were called using the following steps: (i) candidate somatic indels were predicted with GATK Somatic Indel Detector with default parameters; (ii) high confident somatic indels were defined after filtering germline events. All high confident somatic mutations were then filtered out by Single Nucleotide Polymorphism Database (dbSNP; version 135) sites which are commonly polymorphic without known medical impact. The remaining mutations were annotated with ANNOVAR (39) and subjected to subsequent analyses.

Tumor purity and cancer cell fraction estimation

Tumor purity was estimated from FACETS using the somatic mutations and copy-number variations information (40). The cancer cell fraction (CCF) was estimated from somatic SNV frequencies and copy number profiles using PyClone (41). For each sample, the corresponding tumor purity was used to adjust the estimated CCF.

Specifically, the vast majority of somatic SNVs shared by primary and recurrent tumor samples have CCF values larger than 40%, and such a cut-off can also optimally distinguish the clonal and subclonal clusters in the primary- or recurrent-private somatic SNVs. We thus used the 40% CCF as a cut-off value to define clonal versus subclonal SNVs in the neoantigen prediction.

RNA-seq

Total RNA was extracted using the ReliaPrep FFPE Total RNA Miniprep System according to manufacturer's instruction (Promega Corp., catalog no. Z1002). Total 1 μg RNA was used to construct RNA library with the KAPA RNA HyperPrep kit with RiboErase according to manufacturer's instruction (KAPA Biosystems, catalog no. KK8561; Roche Diagnostics). First, Hybridization Oligos (HMR) were used to remove the rRNA. Second, fragmentation buffer was added for interrupting RNA to short fragments. The first-strand and the second-strand cDNA were sequentially synthesized. Then the short fragments were connected with sequencing adaptors, followed by amplification with PCR to prepare the library. The quality and distribution of libraries were analyzed using the the LabChip GX Touch 24 Nucleic Acid Analyzer (PerkinElmer). At last, the library was sequenced using a NovaSeq S4 PE150 instrument (Illumina Inc.) and sequencing was performed using a NovaSeq 6000 S1 Reagent Kit v1.5 (Illumina Inc., catalog no. 20028317).

RNA-seq data analysis for quantifying immune microenvironment

After removing adapters or low-quality reads from the raw data, qualified reads were aligned to the human genome (hg19) by hierarchical indexing for spliced alignment of transcripts with default parameters (40). RSeQC was used to measure gene expression abundance (42), such as immune stimulator gene signature and T-cell inflamed genes (43, 44), as RPKM mapped reads. A curated list of 66 immune markers that encompass cell surface markers of different immune cell populations was collected from the genomic sequencing project of HCC by The Cancer Genome Atlas (TCGA; ref. 45). The comparison of the expression levels of immune-related genes was performed with unpaired *t* test between responders and nonresponders, and between responders without recurrence and nonresponders with recurrence.

HLA type and HLA LOH prediction

To infer the HLA type for each sample, we inputted the BAM file with the aligned RNA-seq reads of normal tissue to POLYSOLVER and employed a Bayesian classifier using default parameters to determine the genotype (46). The LOH events for class I HLA genes were predicted by LOH HLA based on the genotyping result from POLYSOLVER (47). An LOH event for a given HLA allele was determined if the estimated copy number was less than 0.5 and the significance of allelic imbalance was smaller than 0.05.

Immunoediting analysis

Following the method developed by Rooney and colleagues (48), we computed the immunoediting score for each sample. According to Rooney's work, we first constructed the background model of immunoediting using the somatic SNVs of 363 liver hepatocellular carcinoma (LIHC) samples downloaded from TCGA project (TCGA-LIHC; ref. 48). Specifically, we generated 192 mutational spectra based on the WT base, the mutated base, and the nucleotides 1 base upstream and 1 base downstream. For each spectrum, the expected number of nonsilent mutations per silent mutation, $\bar{N}_s$, and the expected number of neoantigens per nonsilent mutation, $\bar{B}_s$, were calculated. Based on these two background rates, we used the number of silent mutations in each tumor sample to predict the number of expected nonsilent mutations, N_{pred}, and the number of expected neoantigens, B_{pred}, under background model in which there is no immunoediting on HLA binders.

$$N_{pred} = \sum_{m}^{Silent\ SNVs} \bar{N}_{s(m)}$$

$$B_{pred} = \sum_{m}^{Silent\ SNVs} \bar{N}_{s(m)}\bar{B}_{s(m)}$$

In the above equations, *s(m)* represents the spectrum of the given mutation. Given that two values, the immunoediting score R is calculated by comparing to the actual counts in the sample, N_{obs} and B_{obs}.

$$R = \frac{B_{obs}/N_{obs}}{B_{pred}/N_{pred}}$$

Specifically, the HLA genotype of each patient in the TCGA- LIHC dataset used for constructing the background model were downloaded from Shukla's study (46).

Tumor mutational burden analysis

Tumor mutational burden (TMB), defined as numbers of mutations per megabase (mb) of genome examined, was detected and quantified with WES data using Johnson method by filtering out driver mutations curated in Catalogue of Somatic Mutations in Cancer (COSMIC) database (49, 50). Mutations likely or known to be bona fide oncogenic drivers and germline polymorphisms were excluded. For patients with more than one tumor nodule, TMB was calculated with their average value.

Neoantigen peptide synthesis

Neoantigen peptides were chemically synthesized by Hanyu Hybio Pharmaceutical Co. using the procedure of solid-phase peptide synthesis, followed by the purification with high performance liquid chromatography. The purity of antigen peptides was over 95%. Lyophilized peptides were reconstituted in sterile saline or DMSO and sterilized in a GMP grade facility, and then frozen at −20°C until use. All peptides were chemically synthesized under GMP conditions.

Neoantigen-loaded DC vaccine and neoantigen-activated T-cell preparation

PBMCs were collected via leukapheresis from each patient and isolated using Lymphoprep (NycomedPharma) before each course of immunotherapy. PBMCs were cryopreserved in liquid nitrogen.

Neoantigen-loaded DC vaccines and neoantigen-activated T cells were manufactured by HRYZ Biotech Co. in a GMP grade facility according to the multi-antigen stimulated cell therapy (MASCT-I) manufacturing protocol (51, 52), which is a therapeutic approach combining tumor antigen peptide–loaded DC vaccines and adoptive transfer of tumor antigen–specific T cells. In brief, monocytes were separated from PBMC using the plastic adherence method, and were cultured in AIM-V (Gibco, #0870112DK) with GM-CSF (1,000 U/mL; Peprotech, #AF-300–03–200) and IL4 (500 U/mL; Peprotech, #AF-200–04–200) for 6 days to differentiate into immature DCs, as previously described (51). On day 5, immature DCs of patients with HCC were pulsed with neoantigen peptides pool (1 μg/mL/peptide) for 24 hours. The DCs were then matured with the cocktail containing monophosphoryl lipid A (MPLA; 5 μg/mL; InvivoGen, #vac-mpls), IFNγ (500 IU/mL; Peprotech, #AF-300–02), and PEG2 (0.3 μg/mL; Cayman Chemical, #14010) for 48 hours to obtain multiple neoantigen-loaded mature DCs.

To prepare the neoantigen-activated T cells, frozen PBMCs were thawed and cocultured with neoantigen-loaded mature DCs in the presence of IL2 (1,000 U/mL; Peprotech, #200–02–250), IL7 (5 ng/mL; Peprotech, #AF-200–07–200), IL15 (5 ng/mL; Peprotech, #AF-200–15–200), IL21 (30 ng/mL; Peprotech, #AF-200–21–1000), and anti-PD1 (15 μg/mL; Camrelizumab, Suncadia Biopharm Co., Ltd.). Anti-CD3 (50 ng/mL; Biogems, #05121–25) was added on day 5 for T-cell expansion. After 2 to 3 weeks, the neoantigen-activated T cells were harvested for i.v. infusion.

Flow cytometry analysis of the infused cells

Before injection into patients, the infused cell products were stained with antibodies against surface markers in stain buffer (BD Biosciences, catalog no. 554656) for 20 minutes at room temperature, followed by fixation with 1% formaldehyde at 4°C for 20 minutes. The cells were then stained using antibodies specific for CD3 (APC/Cy7; BD Biosciences, #557832, SK7), CD4 (FITC; BD Biosciences, #555346, RPA-T4), CD8 (PerCP; Biolegend, #344708, SK1), CD11c (PE, BD Biosciences, #555392, B-ly6), CD86 [FITC, BD Biosciences, #555657, 2331(FUN-1); Supplementary Table S10]. Flow cytometry analysis was performed on a Guava EasyCyte 12HT (MERCK) instrument, and data was analyzed with FlowJo v10 (BD Biosciences).

ELISPOT assay

Blood was collected before resection/RFA to prepare PBMCs as pretreatment baseline, samples of each course were collected by leukapheresis. Patients' PBMCs were first cultured (1×10^6 cells/well) in 96-well plates in AIM-V and stimulated with each neoantigen peptide, including an irrelevant peptide (Ir-pep, HIV-1 ENV, LWDQSLKPCVKLTPLCVTLKCTNVNTTNLN) control for 48 hours. These PBMCs were then transferred to 96-well ELISPOT assay plates (U-CyTech Biosciences; #CT230-PR2) and stimulated again with peptides for another 16 hours for IFNγ detection. The ELISPOT assay was performed according to the manufacturer's instructions. The number of spot-forming units was determined by C.T.L. Immuno Spot S6 Analyzer and analyzed by Immuno Spot v6.0 software. The responses were represented as spot-forming units per 1×10^6 PBMCs/well, and normalized against PBMCs stimulated with irrelevant peptide. The threshold for a positive response was set at a net 50 spots per 1×10^6 cells.

Multiplex immunofluorescence staining

Multiplex immunofluorescence (mIF) staining was performed on 5 μmol/L tissue sections using Pano-7-color panel kit (Panovue, catalog no. 0003100100) following the manufacturer's instructions. Slides were baked at 65°C overnight, dewaxed, rehydrated, fixed in 10% neutral formalin and then washed by ddH_2O for 1 minute (three times). Antigen retrieval was performed using a microwave with EDTA-antigen retrieval buffer (Jiangsu KeyGEN BioTECH, catalog no. KGIHC002) heated to 100°C for 15 minutes. After cooling to room temperature, slides were washed with ddH_2O for 1 minute, and then washed with TRIS-buffered saline with Tween 20 (TBST) for 2 minutes and blocked with 20% blocking buffer (normal goat serum diluted in PBS, Bioss, catalog no. C01–03001) for 10 minutes at room temperature. Slides were incubated with primary anti-human CD8 (1:200, Abcam) at 37°C for 30 minutes. Slides were washed with TBST for 3 minutes (three times) and incubated with secondary antibody (Panovue, catalog no. 0003100100) for 10 minutes at room temperature. Slides were washed with TBST for 3 minutes (three times) and stained with Opal-650 (1:100, Panovue, catalog no. 0003100100) for 10 minutes at room temperature. Multiplex staining was performed by repeating staining cycles with microwave heating between each step to remove the antibody complex. Successive antibodies and incubating time were as followed: CD68 (1:200, CST, 37°C, 30 minutes, Opal-620, 1:100); granzyme B (1:100, Abcam, 37°C, 30 minutes, Opal-540, 1:100); CD11c (1:500, Abcam, 37°C, 30 minutes, Opal-690, 1:100); PD-1 (1:200, Abcam, 4°C, overnight, Opal-560, 1:100); CD4 (1:200, Abcam, 37°C, 60 minutes, Opal-520, 1:100). Secondary antibodies (Panovue, catalog no. 0003100100) were incubated for 10 minutes at room temperature. Nuclei were stained with DAPI 1:200 for 10 minutes (Panovue, catalog no. 0003100100), washed, and mounted with mounting medium (Panovue, catalog no. 0003100100). Details on the antibodies used and the antibody order, dilution, and fluorophore pairing for the panel described here are in Supplementary Tables S10 and S11. Upon completion of staining, slides

were scanned using TissueFAXS Spectra imaging system (TissueGnostics).

Statistical analysis

Continuous variables were described as medians (interquartile ranges) or means (SDs). Categorical variables were described as numbers (percentages). DFS was described by Kaplan–Meier method and tested by log–rank method. The immune marker gene, immune cell density, TMB, and observed/expected neoantigen ratio between groups of response and nonresponse, and between groups of response without recurrence and nonresponse with recurrence were compared by unpaired *t* test. All analysis was conducted by Stata/MP 14.0 software. Statistical significance was defined as a two-sided *P* of less than 0.05.

Data availability

The RNA-seq data reported in this paper have been deposited in the Genome Sequence Archive in National Genomics Data Center, Beijing Institute of Genomics (China National Center for Bioinformation), Chinese Academy of Sciences (Beijing, China), under accession number HRA001902. All other data generated in the study are available in the article and its supplementary files or from the authors upon reasonable request.

Ethics approval and consent to participate

The study was performed in accordance with the Declaration of Helsinki and was approved by the institutional ethics committee for Clinical Research and Animal Trials of the First Affiliated Hospital of Sun Yat-sen University. All patients provided written informed consent both before enrollment and before registration.

Results

Patients

From September 25, 2017, to November 26, 2018, 23 patients were enrolled prior to curative resection/RFA. Eight patients were excluded due to poor compliance and not enrolled into the trial, and 15 patients were assessed before the combination immunotherapy. Five patients were excluded due to the pathologic diagnosis of non-HCC ($n = 4$) or an inadequate number of predicted neoantigen peptides less than 10 ($n = 1$). Ten patients received the adjuvant combination immunotherapy (**Fig. 1A**). Nine of the 10 patients were male, and the median age at the time of enrollment was 57.6 years (range, 36.4–75.4 years). Nine patients had a solitary tumor with a diameter between 2.1 cm and 4.8 cm, and 1 patient had two tumors measuring 1.4 cm and 2.4 cm in diameter, respectively. Among the 10 patients, three received RFA, and the other 7 underwent surgical resection. The median number of adjuvant combination immunotherapy cycles was 12 (range, 3–21). All patients received the adjuvant combination immunotherapy as per protocol (1.65×10^6–18.8×10^6 DC cells and 0.56×10^6–8.12×10^9 neoantigen-activated T cells per infusion). The median time between the curative treatment and the first cycle of adjuvant neoantigen-loaded DC infusion and ACT was 16.6 weeks (range, 14.3–25.0 weeks) and 20.2 weeks (range, 17.9–25.7 weeks), respectively. The patient characteristics are summarized in Supplementary Table S12.

Therapeutic peptides, neoantigen-loaded DC vaccine, and neoantigen-activated T cells

The proportion of the identified neoantigen peptides that were eventually administered was 77.7% (80/103), due to the exclusion of peptides that were difficult to synthesize; and the final number of administered peptides for each patient varied from 5 to 11 (Supplementary Table S13). Before cell infusions, we assessed the cell composition of the infusion product by flow cytometry. For infusion of DCs, $CD11c^+$ DCs accounted for 72.3% of live mononuclear cells on average, of which 64.9% were $CD11c^+CD86^+$ DCs. For infusion of lymphocytes, the average percentages of $CD3^+$ T cells, $CD3^+CD4^+$ T cells, and $CD3^+CD8^+$ T cells were 94.7%, 22.7%, and 64.7%, respectively (Supplementary Fig. S3).

Preclinical safety evaluation

To test the safety of the combination immunotherapy, we injected LW2011–01 (T cells) subcutaneously and LW2011–02 (DCs) intravenously into NOD-SCID mice following the experimental design shown in Supplementary Fig. S2). Grouping and dosage are summarized in Supplementary Table S1. Body weight was monitored at different time points and was not affected by low dose of combination immunotherapy (two times of clinical dose) but slightly decreased in male mice of high dose group (five times of clinical dose; Supplementary Table S2). Hematologic parameters, circulating cell populations, coagulation parameters, blood biochemical profiles were also monitored after treatment. No severe toxicity nor treatment-related deaths were observed (Supplementary Tables S3–S9).

Adjuvant combination immunotherapy induces neoantigen-specific, durable T-cell responses

Neoantigen-specific T-cell responses against immunizing peptides (IMP; Supplementary Table S13) were detected by *ex vivo* IFNγ ELISPOT assay at the beginning of the study (before RFA or surgery; except for patients 6 and 7) and at the end of every course of the adjuvant combination immunotherapy (**Fig. 2A**). As shown in **Fig. 2B**, 42.5% of the adopted and administered peptides generated immune responses, and 76.5% of the response represented a *de novo* immune response that did not exist before adjuvant combination immunotherapy. Among the 10 participants, 7 (70%; patients 3, 4, 5, 6, 7, 8, and 9) had an immune response against multiple predicted epitopes and were referred to as responders, while the other 3 (patients 1, 2, and 10) did not generate IFNγ responses to stimulation with adopted peptides during the treated courses and were referred to as nonresponders (**Fig. 2A** and **B**; Supplementary Fig. S4A). Minimal neoantigen-specific T-cell responses were observed after resection or RFA but before adjuvant combination immunotherapy in patients 1, 3, 5, 6, 7, 8, and 9 (**Fig. 2A**; Supplementary Fig. S4A), suggesting that resection or RFA might induce weak neoantigen-specific immunity. After adjuvant combination immunotherapy, responses against neoantigens were enhanced when compared with prevaccination in all 7 responders (**Fig. 2C**; Supplementary Fig. S4B). In patient 6, *ex vivo* responses to IMPs were undetectable before therapy but became readily detectable after, indicating the *de novo* generation of effective neoantigen-specific T-cell responses as a result of adjuvant combination immunotherapy (**Fig. 2D**; **Fig. 3A**). Moreover, for responding patients 6 and 7, the ELISPOT assay showed that neoantigen-specific immune responses were present even at 3 months after the completion of the therapy (**Fig. 3B** and **C**).

We reasoned that adjuvant combination immunotherapy might induce a broadened antitumor immunity (antigen spreading) in which T-cell responses could be induced against other neoantigen peptides that were identified but not administered as part of the therapy [spreading peptides (SP)]. To assess whether antigen spreading occurred after the immunotherapy, we tested the immune responses to peptides that were highly ranked but were not used for immunization in 4 patients (patients 4, 6, 7, 8). *Ex vivo* responses to SPs were

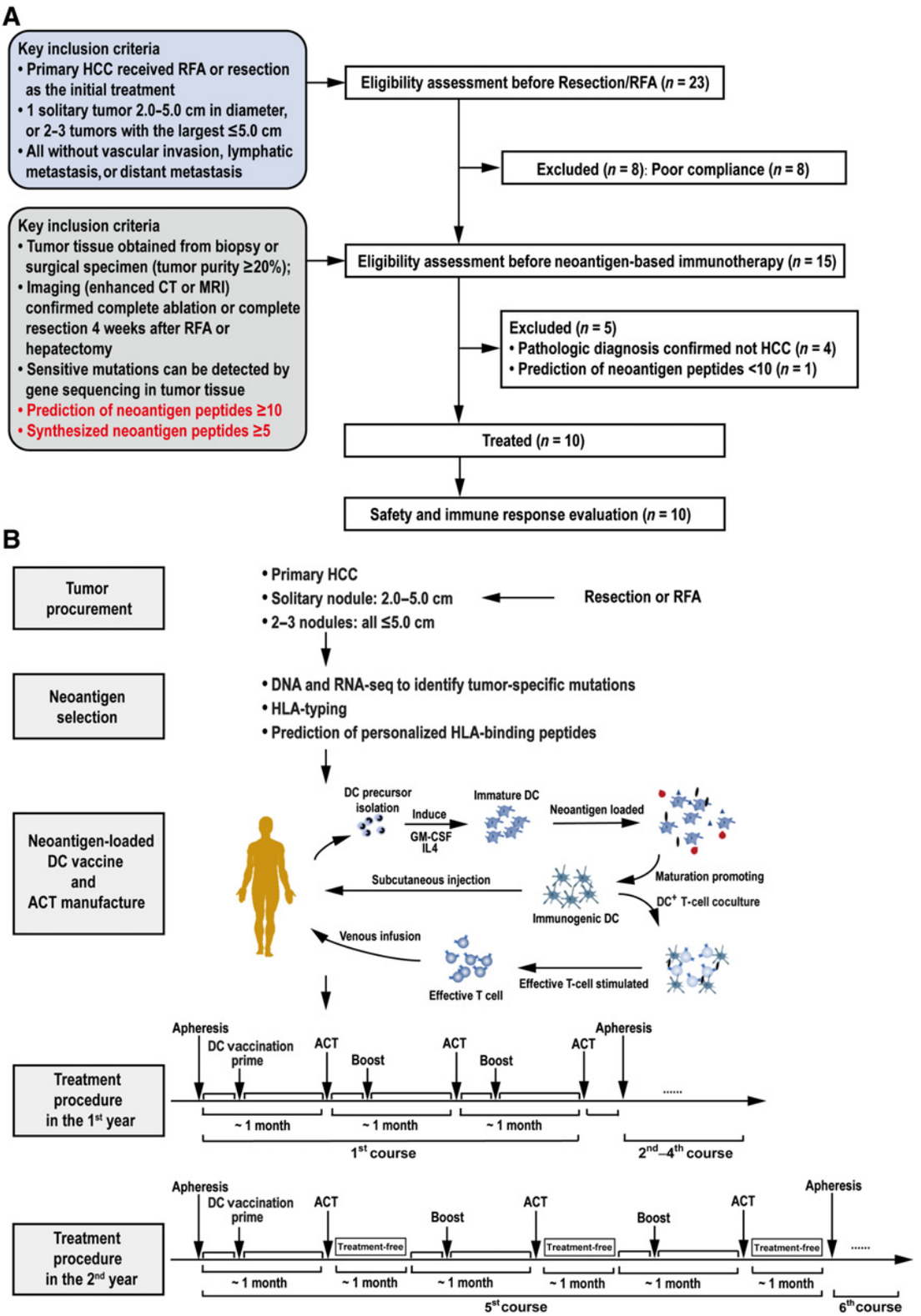

Figure 1.
Schematic showing patient enrollment and study design. **A,** Flow chart showing patient enrollment; **B,** Schematic of vaccine design, manufacturing, and clinical study procedure.

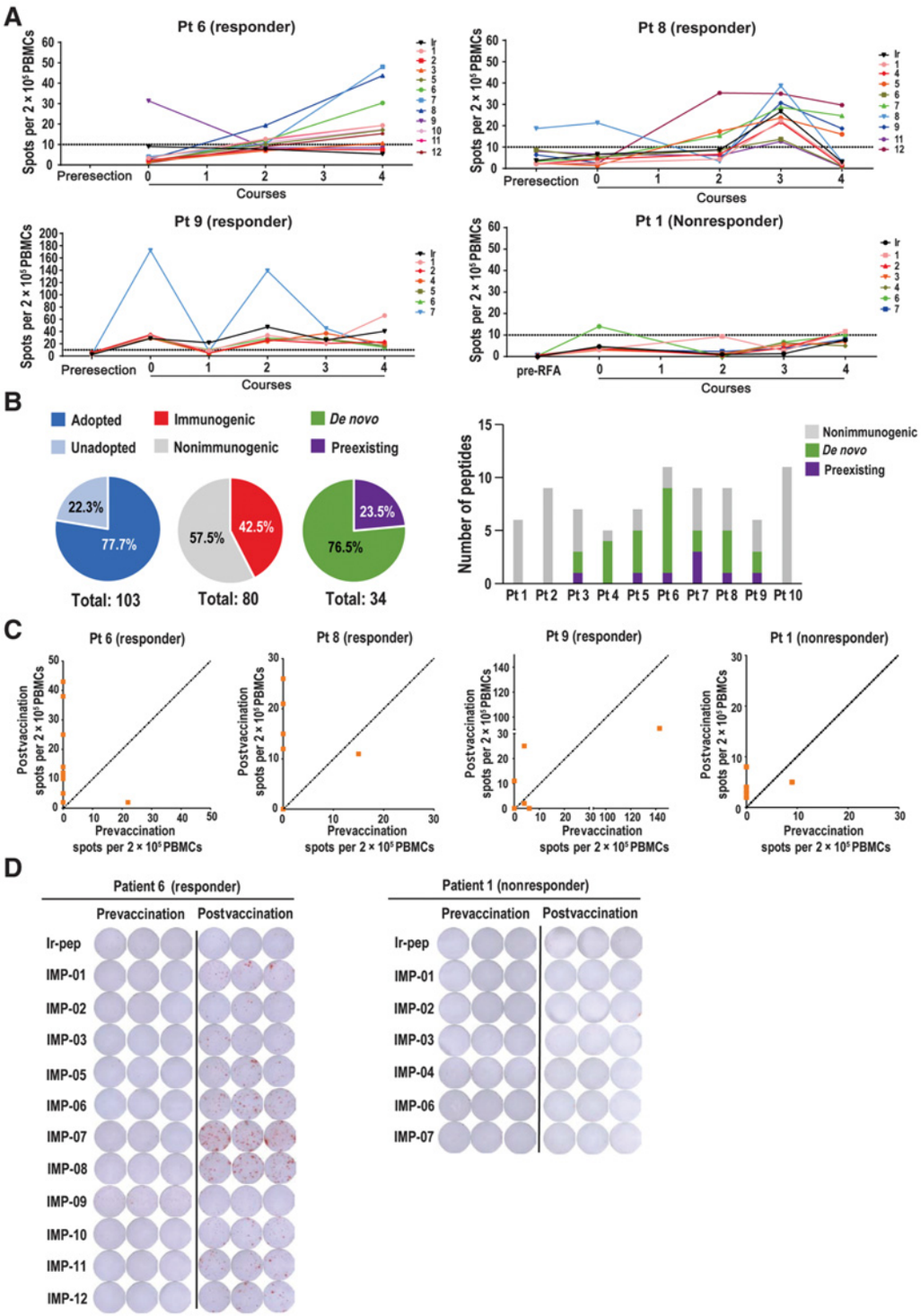

Figure 2.

Immune activation of T cells by neoantigen-loaded DC vaccine and neoantigen-activated T-cell transfer in patients with HCC. **A,** The dynamic responses of PBMCs to IMP by *ex vivo* IFNγ ELISPOT for 4 representative patients, including 3 responders (patients 6, 8, and 9) and 1 nonresponder (patient 1) with duplicate or triplicate wells for each sample [irrelevant peptide (Ir-pep)]; **B,** Statistics of T-cell response in IFNγ ELISPOT assay for all 80 vaccination neoantigen peptides on cohort level (left) and individual patient (right); **C,** Pre- versus postvaccination responses to IMPs for 3 representative responders (patients 6, 8, and 9) and 1 representative nonresponder (patient 1). The highest value of postvaccination response to IMP was selected from ELISPOT assays in different vaccination cycles; **D,** Pre- versus postvaccination responses to IMP examples. The statistical data are presented as mean. Pt, patient.

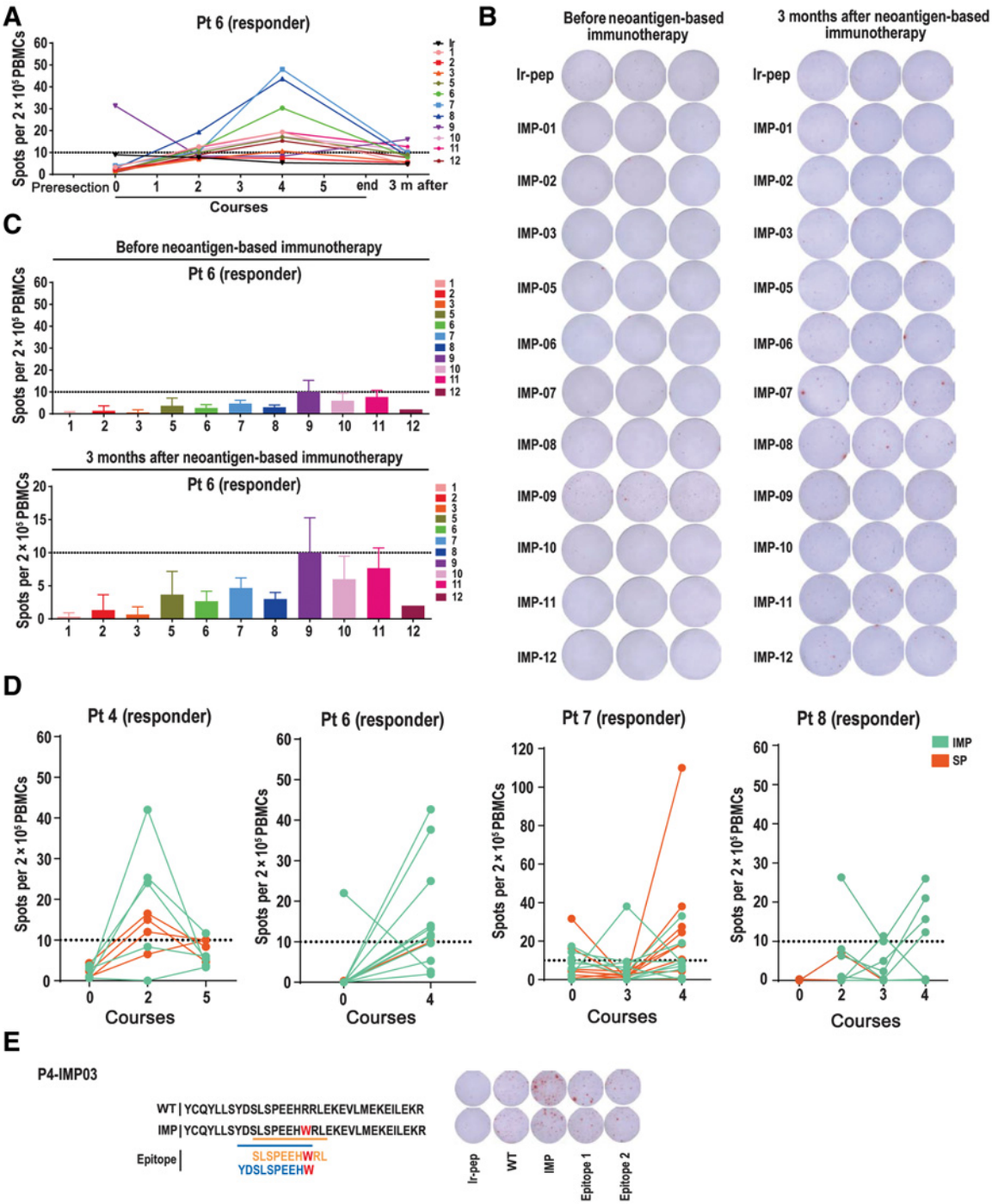

Figure 3.

Adjuvant neoantigen-based combination immunotherapy induced sustainable neoantigen-specific immunity and epitope spreading. **A,** A sustainable immune response to neoantigen peptides was observed 3 months after the end of treatment. The dynamic responses of PBMCs to IMPs by *ex vivo* IFNγ ELISPOT for patient 6, including the responses 3 months after the completion of the combination immunotherapy. IFNγ secretion by PBMCs after IMP-09 stimulation 3 months after the end of the treatment was indirect proof of the existence of memory T cells (with a positive threshold ≥50). **B** and **C,** Comparison of the IFNγ responses of PBMCs against individual IMPs for patient 6 before and after adjuvant combined immunotherapy. No immune response was detected for patient 6 before the combined immunotherapy, whereas an immune response to IMP-09 was detected 3 months after the combined immunotherapy. **D,** Antigen spreading was observed after adjuvant combined immunotherapy. Multiple patients (patient 4, 6, 7, 8) showed a relatively strong immune response in the whole trial. Their PBMC responses to other neoantigens (SP) that were not used for immunization were checked by ELISPOT assay. In patients 4 and 7, PBMC responses to SPs showed a trend similar to that of IMPs in the selected vaccination cycles (with positive threshold ≥50). **E,** WT peptide cross-reactivity of postvaccination PBMCs in patient 4. Pt, patient; m, months.

detected in 3 out of 4 tested immune responders (75%; patients 4, 6, and 7; **Fig. 3D**), suggesting that neoantigen-based combination immunotherapy indeed induced antigen spreading in the responding patients. In patients 4 and 6, *ex vivo* responses were detected for all the tested SPs, whereas in patient 7, *ex vivo* responses were detected for 77.8% of the tested SPs. All these responses to SPs were *de novo*, and showed a trend similar to that of IMPs in the selected vaccination courses (**Fig. 3D**). The immune responders with antigen spreading were all tumor-free for at least 2 years after curative treatment. We further used the corresponding predicted 8- to 11-mer MHC class I epitope peptides (EPT) in the IMPs to stimulate PBMCs and determine the $CD8^+$ T-cell response in responders (patients 3, 4, 5, 6, 7, 8, and 9). We found that responses against multiple EPTs were observed in 4 responders (patients 3, 4, 7, and 8; Supplementary Fig. S5), suggesting the generation of multiclonal $CD8^+$ T-cell responses. To determine the specificity of these responses, PBMCs were loaded exogenously with mutated or WT peptides. In patient 4, preferential reactivity to the mutated peptides compared with the corresponding WT peptide was observed (**Fig. 3E**).

Safety and clinical outcomes

The median follow-up time after curative treatment was 28.3 (IQR = 26.3–33.9) months. There were no grade ≥3 treatment-related AEs or treatment-related deaths in the study, indicating that the adjuvant combination immunotherapy was safe. Six out of 10 patients developed grade 1 or 2 treatment-related AEs (Supplementary Table S14). The observed AEs included vomiting ($n = 1$, 10.0%), coughing ($n = 4$, 40.0%), gum bleeding ($n = 2$, 20.0%), pain ($n = 1$, 10.0%), itchiness ($n = 1$, 10.0%), dizziness ($n = 5$, 50.0%), tinnitus ($n = 1$, 10.0%), abdominal pain ($n = 1$, 10.0%), thrombocytopenia ($n = 1$, 10.0%), anaphylactic reaction ($n = 1$, 10.0%), allergic rhinitis ($n = 2$, 20.0%), and balanitis ($n = 1$, 10.0%).

The patient outcomes are summarized in Supplementary Table S15. Among the 10 patients, five (50%; patients 4, 6, 7, 8, and 9) did not relapse for 2 years after curative treatment (**Fig. 4A**). Median DFS was 18.3 months [95% confidence interval (CI), 4.9–NA; **Fig. 4B**]. Patients with an immune response had significantly longer DFS than patients without a response (log–rank $P = 0.012$; **Fig. 4C**). 71.4% of the immune responders did not relapse for 2 years after curative treatment whereas all 3 nonresponders developed recurrence and 1 died. Moreover, patients with antigen spreading had significantly prolonged DFS compared with those who did not have antigen spreading (log–rank $P = 0.019$; **Fig. 4D**). Among the 5 patients with recurrence, 3 (patients 1, 2, and 10) were immune nonresponders. Nonresponding patient 1 developed *de novo* multiple intrahepatic recurrences just after 10 cycles of adjuvant treatment. Nonresponding patient 2 also developed multiple intrahepatic recurrent tumors and portal vein thrombus after seven cycles of adjuvant treatment, making further curative treatments impossible; combination therapy (TACE and sorafenib) was given. This patient died due to rapid tumor progression 3 months after recurrence. Nonresponding patient 10 relapsed very quickly (true recurrence) after one cycle of adjuvant treatment and underwent surgical resection for the recurrent tumors. Unfortunately, they developed another two recurrences within a year. Collectively, these observations appear to suggest that patients without immune response are more likely to develop early and multiple recurrences.

Tumor mutational burden and high immune cell infiltration are associated with an immune response

To better identify patients who may respond to or benefit from the adjuvant combination immunotherapy, we stratified patients into four categories according to immune response and clinical outcome: immune responders, immune nonresponders, nonresponder with recurrence, and responder without recurrence. In these four categories, we analyzed TMB, immunogenomic profile, immune gene expression signature, immune cell infiltration using WES data, RNA-seq data, and mIF staining of serial tumor tissue samples (primary and recurrent tumors) to identify factors associated with patients' immune response and/or recurrence.

First, TMB was found to be significantly higher in the primary tumors of the responders without recurrence than in the tumors of the nonresponders with recurrence ($P = 0.018$, Supplementary Fig. S7A). Then, we calculated the immunoediting score in the primary tumors of the above four categories to compare the possibility of neoantigen depletion, where a lower score indicated a higher likelihood of neoantigen presentation impairment and immune evasion (48, 53). The immunoediting score tended to be lower in the primary tumors of the nonresponders than in the primary tumors of the responders (median: 1.9 vs. 3.9, $P = 0.45$; Supplementary Fig. S7B). Similarly, the immunoediting score in the primary tumors of patients with recurrence was also lower than that in the primary tumors of patients without recurrence (median: 1.9 vs. 3.9, $P = 0.57$; Supplementary Fig. S7C). Although it did not reach statistical significance, the primary tumors of the nonresponders presented a tendency to neoantigen depletion.

In addition to the genome, the tumor microenvironment is associated with immunotherapy response (54). To characterize the immune microenvironment of the primary tumors across different patient categories, immune gene expression analysis and mIF staining were performed. We compared the immune functional genes between the responders and nonresponders (43, 54, 55, 56), and between responders without recurrence and nonresponders with recurrence. Tumors in the responder category showed higher expression of an immune stimulator signature than tumors in the nonresponder category ($P = 0.049$; ref. 43), suggesting that the immunity of the tumors for the responders was more active and partially explained the immune response for these patients (**Fig. 5A**; Supplementary Fig. S8A). Similarly, the primary tumors of the responders without recurrence expressed marginally higher expression of the immune stimulator signature ($P = 0.066$) than those of nonresponders with recurrence (**Fig. 5A**; Supplementary Fig. S8B). Moreover, we found that the responders with or without recurrence exhibited a tendency to higher levels of the T-cell–inflamed gene expression profile (**Fig. 5B**). This is related to antigen presentation, chemokine expression, cytotoxic activity, and adaptive immune resistance, and closely correlated with immunotherapy in multiple solid malignancies (44).

Next, we tried to evaluate distinct immune cell infiltrations associated with neoantigen presentation and antitumor immunity, including DCs, T cells, and myeloid cells, in primary tumors. mIF staining with markers of DCs, T cells, macrophages, and their functional states showed more infiltration of $CD11c^+$ DCs ($P < 0.05$), $CD8^+$ cytotoxic T cells ($P < 0.05$), and granzyme B^+ cells ($P = 0.0873$) in the primary tumors of responders without recurrence compared with those of nonresponders with recurrence (**Fig. 5C** and **D**). Collectively, these data suggest that high TMB, high infiltration of DC and $CD8^+$ T cells, and high T-cell–inflamed gene expression profile score in primary tumors were associated with the positive immune response and good prognosis of patients receiving this adjuvant combination immunotherapy.

Recurrent tumors escape immune surveillance through neoantigen depletion

Immune evasion mechanisms such as immunoediting, HLA-LOH, and mutation of genes in the antigen-presenting pathway are reported

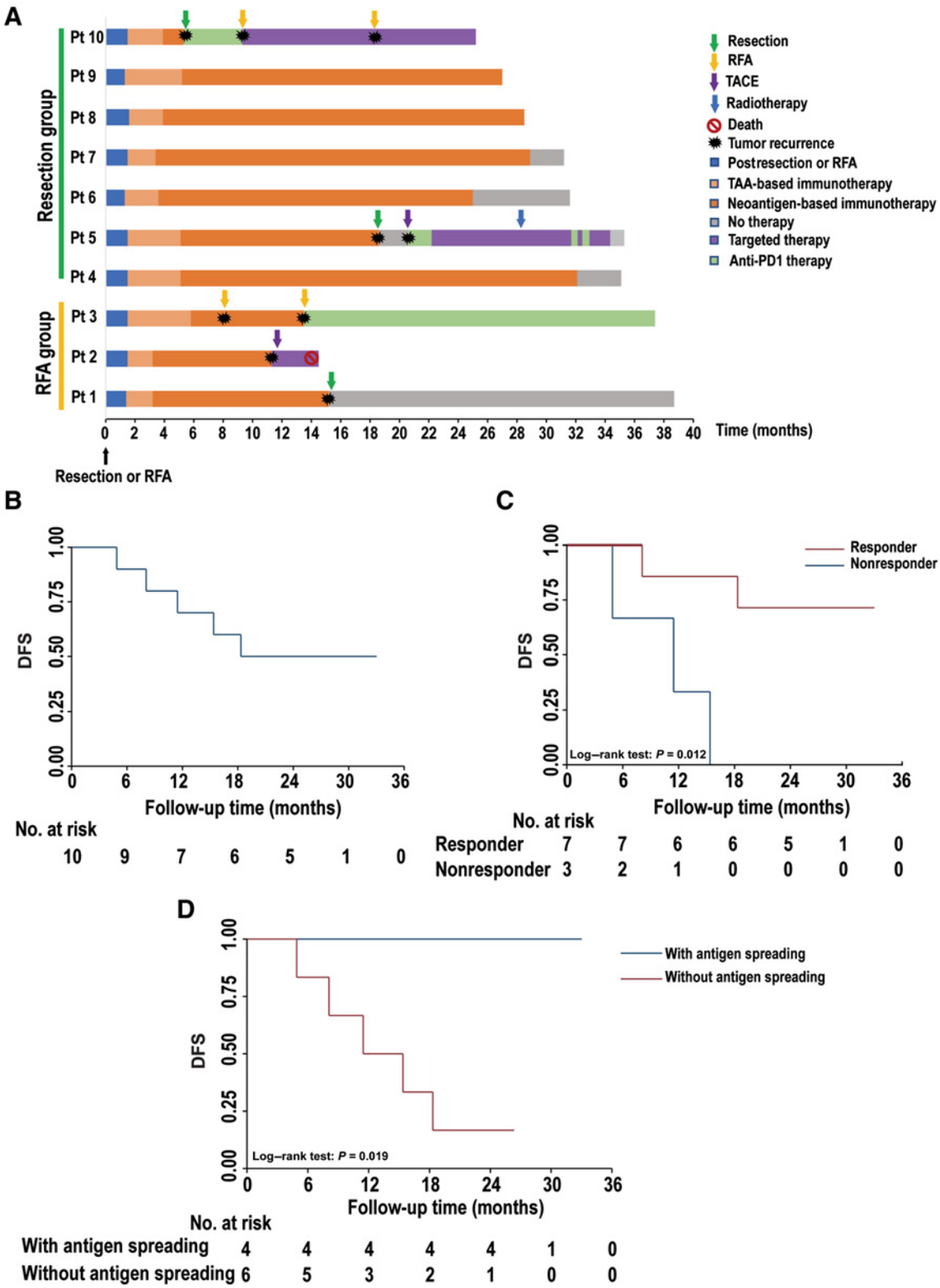

Figure 4.

Clinical outcomes of patients with HCC treated with adjuvant combination immunotherapy after resection or RFA. **A,** Clinical event timeline for 10 patients administered adjuvant combination immunotherapy after surgery or RFA; **B,** Kaplan–Meier survival curves of DFS for all the patients; **C,** Kaplan–Meier survival curves for patients with or without immune response (log-rank test was used); **D,** Kaplan–Meier survival curves for patients with antigen spreading or without antigen spreading (log-rank test was used). Pt, patient.

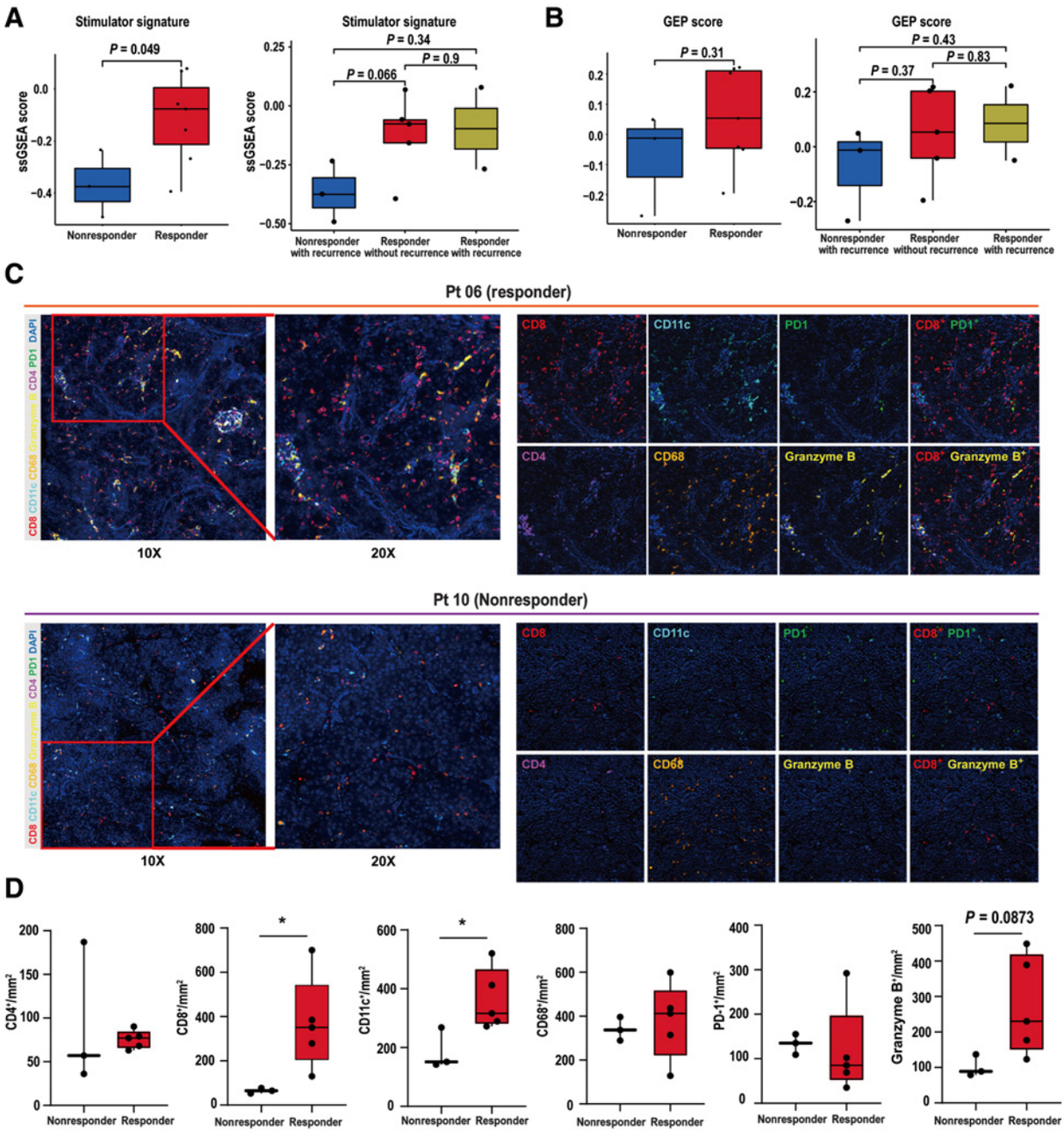

Figure 5.

The immune landscape of primary HCC with different outcomes after adjuvant combination immunotherapy. **A,** Comparison of the expression of an immune stimulatory signature between responders ($n = 7$) and nonresponders ($n = 3$; left), and among responders without recurrence ($n = 5$), nonresponders with recurrence ($n = 3$), and responders with recurrence ($n = 2$; right); **B,** Comparison of the T-cell–inflamed gene expression signature (GEP score) between responders ($n = 7$) and nonresponders ($n = 3$; left), and among responders without recurrence ($n = 5$), nonresponders with recurrence ($n = 3$), and responders with recurrence ($n = 2$; right); **C,** Representative images of multiple immunofluorescences staining for CD4, CD8, CD11c, CD68, PD1, and granzyme B in a responder without recurrence (patient 6; top) and a nonresponder with recurrence (patient 10; bottom). **D,** Comparison of the cell densities for $CD4^+$, $CD8^+$, $CD11c^+$, $CD68^+$, granzyme B^+, PD-1^+ cells between responder without recurrence and nonresponder with recurrence. Nonpaired *t* test was performed. $P < 0.05$. ssGSEA, single sample gene set enrichment analysis.

to decrease neoantigen presentation and thus are inversely associated with the immunotherapy response and survival outcome (57, 58). In our study, 5 patients developed recurrence during the adjuvant combination immunotherapy. To explore potential mechanisms linked to tumor recurrence under the combination immunotherapy pressure, we investigated whether the abovementioned immune evasion mechanisms could be observed in our cohort. Core mutated genes in the antigen-presenting pathways, such as the *B2M* gene, were not

detected for either the primary or recurrent tumors. The proportion of HLA-LOH events was only 16% (4/25) in all the tumor samples and 9.1% (1/11) in the recurrent tumor samples (Supplementary Fig. S9), suggesting that HLA-LOH was also not a major factor contributing to the recurrence of HCC after adjuvant combination immunotherapy. However, we found that the immunoediting score of most recurrent tumor samples was lower than 1 (**Fig. 6A** and **B**), which was also significantly lower than those of primary tumor samples (7/9 vs. 1/17, $P = 0.014$), suggesting that neoantigen depletion occurred in the recurrent tumors. Moreover, we further analyzed the dynamic changes in the CCF of immunogenic (neoantigen) clones from paired primary and recurrent tumors in 3 recurrent patients with paired tumor samples. It demonstrated that the CCF of immunogenic clones tended to be lower in the recurrent tumors than in the paired primary tumors (i.e., cluster 0 in patient 1; clusters 0 and 1 in patient 5; and clusters 1, 2, 3, and 9 in patient 10), and that the immunogenic clones of the recurrent tumors could be newly generated clones that were not present in the paired primary tumors (cluster 1 and 2 in patient 1, cluster 0 in patient 10; **Fig. 6C**). Together this suggested that neoantigen depletion and generation of *de novo* immunogenic clones might be associated with immune evasion and tumor recurrence under the pressure of adjuvant combination immunotherapy.

Discussion

In this trial, the personalized neoantigen vaccine plus neoantigen-activated T-cell therapy we tested was demonstrated to be feasible and safe. The adjuvant combination immunotherapy induced sustained neoantigen-specific immunity and antigen spreading. Immune responders to this immunotherapy yielded an improved DFS compared with nonresponders. However, due to the small sample size at this stage of the study, these promising findings require validation from a large-scale randomized-controlled trial (RCT) with a comparator cohort.

Our neoantigen-based combination immunotherapy successfully induced the generation of multiclonal $CD8^+$ T cells and specific anti-HCC immune responses in 70% of the treated patients. We believe that the major reason for achieving such a high immune response rate is the use of rationally selected, personalized neoantigens for vaccination. In our study, we not only used NetMHCpan4.0 to predict the binding affinity of the peptide, but also added NetMHCStabPan to predict the peptide-binding stability, which we consider an important method to improve the accuracy of neoantigen selection. Our approach is substantially different from that of Carreno and colleagues, where T2 assay or fluorescence polarization assay was used to confirm the peptides binding by HLA-A*02:01 (21).

Our results show that 76.5% of the responses were *de novo* immune responses, indicating that the neoantigen peptides successfully induced neoantigen-specific immune responses that were not present in the patients before the combination immunotherapy. Concordantly, several previous personalized neoantigen vaccines have also stimulated *de novo* responses (20, 22, 23). The induced *de novo* T-cell clones with tumor-antigen specificity help eliminate the tumor cells, and have been reported to be associated with better clinical outcomes. Moreover, immune responses to spreading peptides were also detected, which indicated that our adjuvant combination immunotherapy broadly enhanced patients' antitumor immunity that was not restricted to the targeted therapeutic peptides. Similarly, two previous studies relevant to neoantigen vaccine also reported the phenomenon of epitope spreading (23, 59). This finding is clinically important as it implies that neoantigen-induced T cells are not only able to traffic to the tumor, but also able to kill the tumor cells, resulting in the release of additional nontargeted neoantigens that become targets for additional T cells. It also suggests the possibility that it may only require targeting a subset of neoantigens to induce a broad immune response against the expressed neoantigens (59). The occurrence of epitope spreading may help target tumor cells that do not carry truncal neoantigens and thus might be a mechanism to control tumor heterogeneity (5). Consistent with this, the subset of patients with epitope spreading exhibited a significantly prolonged DFS compared with those without it in our cohort. In addition, we observed that immune responses were already established after resection/RFA and before immunization in some patients (1, 3, 5, 6, 7, 8, and 9), despite the fact that these responses were relatively weak. This finding implies the possibility of neoantigen release and effective stimulation of host T cells due to resection/RFA, as long hypothesized in the field (15). It provides a rationale for combining adjuvant immunotherapy after resection/RFA to further enhance neoantigen exposure and specific antitumor immunity in HCC, which also partly explains the efficacy of our adjuvant combination immunotherapy after resection/RFA.

In addition to inducing a high immune response rate, another advantage of using neoantigens is a very favorable safety profile. All treatment-related AEs in our study were Common Terminology Criteria for Adverse Events (CTCAE) grade 1 or 2, and there was not a single severe event observed. With this favorable safety profile, our adjuvant combination neoantigen-based immunotherapy was successfully administered to all the included patients without unexpected delay, establishing the feasibility of this treatment in clinical practice. Concern about the specificity of TAAs has been raised in previous reports about HCC vaccines, given that some TAAs are expressed not only by tumors but also in normal tissue, which may induce unexpected organ damage to some extent (19). Our personalized neoantigen-based immunotherapy addressed this problem by using neoantigens to selectively target specific tumors relative to healthy tissues. This aims to improve the specificity and efficacy of immunotherapy while guaranteeing safety without other organ damage. It is tempting to speculate that the low rate and grade of side effects of our combination immunotherapy also carry the additional advantage of preserving liver function; this may provide a flexibility to combine such immunotherapy with other adjuvant antirecurrence therapies and may consequently play an important role in improving the long-term outcomes.

Besides the precise use of neoantigens, the combination of a DC vaccine (a therapy of active immunization) and ACT might also contribute to the high rate of immune response and improved survival for our patients. DC vaccines are able to increase the proportion of tumor neoantigen exposure, activate host antigen-specific T cells, and accelerate T-cell homing and therefore are important in maintaining long-term antitumor immunity (14, 21, 27). However, DC vaccines cannot induce a large number of antitumor T cells in a short period of time, and their efficacy might be restricted due to potential issues of the immunosuppressive microenvironment and T-cell dysfunction (24, 60). ACT can immediately supplement a large number of tumor-specific activated T cells in patients. For HCC, a malignancy with high rates of early and late recurrence, both short-term and long-term antitumor immune responses are required to prevent tumor recurrence. Therefore, we reason that in theory, combining DC vaccines and ACT should achieve strong short-term and long-term treatment effects by mutual complementation and synergistic effects. In our study, a sustained neoantigen-specific immune response was detected at 3 months after the end of adjuvant combination

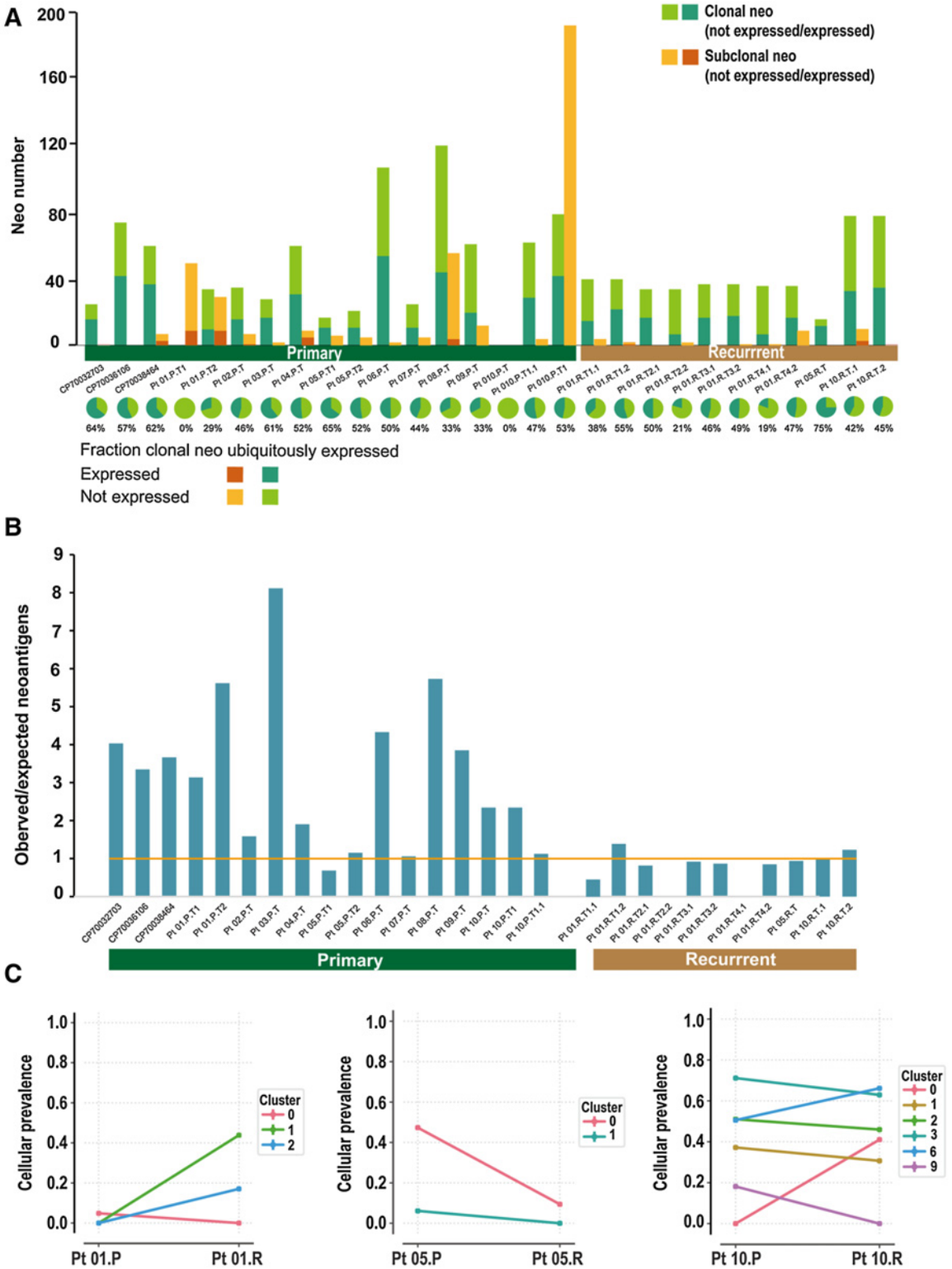

Figure 6.

Immune escape through immunoediting in recurrent tumors under treatment pressure from adjuvant combination immunotherapy. **A,** Top, the number of clonally and sub clonally expressed neoantigens is presented at the patient level. Bottom, the fraction of clonal neoantigens that are ubiquitously expressed. **B,** Comparison of the observed/expected neoantigen ratio (immunoediting score) between primary and recurrent HCC. **C,** The dynamic changes in the cancer cell fraction of immunogenic clones from paired primary tumors to recurrent tumors in 3 patients with recurrent HCC with paired tumor samples. Pt, patient.

immunotherapy, implying the presence of memory T cells capable of providing a long-term immune protection (or related to prolonged survival) to the patients. Consistent with this, the DFS of the immune responders was significantly better than that of the nonresponders. When compared with the survival data of patients with HCC with similar baseline characteristics who underwent local therapy alone during the same period in our center, the immune responders receiving adjuvant immunotherapy in our study tended to have a higher 2-year DFS rate (71.4% vs. 60%). These data support the potential of the combination immunotherapy based on neoantigens in helping to prevent HCC recurrence. Our study may help pave the way for further development of cell-based immunotherapy for high-heterogeneity solid cancers such as HCC. However, due to the small sample size of this study, our findings, while promising, should be considered hypothesis-generating and further verification is needed.

To further explore the biomarkers associated with the patients' immune response and tumor recurrence under the scenario of neoantigen-based immunotherapy, we compared the immunogenomic profiles and immune cell infiltration between responders and nonresponders, and between responders without recurrence and nonresponders with recurrence. In the responder category, we observed a higher expression of immune-related markers, more immune cell infiltration (i.e., $CD8^+$ T cells) and upregulation of the T-cell–inflamed gene expression pattern that correlated with antigen presentation, chemokine expression, cytotoxic activity, and adaptive immune resistance (37). All of these factors reflect a "hot" immune state of the responders' tumors which correlated with antitumor immune response and better survival outcomes. Moreover, a higher TMB was found in those patients who had an immune response. These data collectively demonstrate that a "hot" immune state and high TMB could serve as indicators of a positive immune response for adjuvant combination immunotherapy in HCC. On the other hand, for patients with recurrence, we tried to evaluate whether any immune evasion mechanism occurred during the evolution from primary to recurrent HCC. Neoantigen depletion (immunoediting) was found in recurrent tumors, and the immunogenic clones of the recurrent tumors could be newly arising that did not exist for the paired primary tumors, suggesting that immune evasion occurs under the treatment pressure of the combination immunotherapy. Under such a circumstance, the combination immunotherapy based on the neoantigens of the primary HCC might fall short of controlling the recurrent HCC with reduced neoantigens and *de novo* neoantigens. These observations associated with immune evasion under the treatment pressure of immunotherapy will guide future design of immunotherapies to overcome such challenges.

Our study had several limitations. First, we tested the combination immunotherapy in patients receiving RFA or resection, and could not provide the comparison results for these two different curative treatments due to small sample size. However, several RCTs and large-scale cohort studies (60–64) have shown that the overall survival and recurrence-free survival between RFA and resection are comparable without significant difference for tumors within the inclusion criteria of our trial, and thus we think this influence might be acceptable. The comparison of neoantigen-based combination immunotherapy in patients who underwent RFA or resection requires further larger RCTs to investigate. Second, due to the small sample size, our promising findings warrant further validation in our ongoing RAMEC study with a comparator cohort. Third, most of our study subjects had Hepatitis B virus–related HCC, and the role of our treatment in HCC with other etiologies cannot be evaluated.

This is, to our knowledge, the first prospective clinical trial to evaluate the feasibility, safety, and efficacy of an adjuvant combination treatment of neoantigen-loaded DC vaccine and neoantigen-activated T-cell therapy in patients with HCC undergoing curative treatments. Our study provides insight into the potential efficacy of neoantigen-based combination immunotherapy as an adjuvant treatment for patients with HCC to induce anti-HCC immunity and prevent HCC recurrence.

Authors' Disclosures

Y. Han reports other support from HRYZ Biotech Co. outside the submitted work. L. Tang reports other support from HRYZ Biotech Co., outside the submitted work. Y. Ma reports other support from HRYZ Biotech Co. outside the submitted work. X. Li reports grants from HRYZ Biotech Co. outside the submitted work. No disclosures were reported by the other authors.

Authors' Contributions

S. Peng: Conceptualization, data curation, supervision, funding acquisition, investigation, methodology, writing–original draft, project administration, writing–review and editing. **S. Chen:** Conceptualization, data curation, investigation, writing–original draft, writing–review and editing. **W. Hu:** Data curation, formal analysis, methodology, writing–original draft, writing–review and editing. **J. Mei:** Data curation, investigation. **X. Zeng:** Data curation, formal analysis, investigation, methodology, writing–original draft, writing–review and editing. **T. Su:** Data curation, writing–original draft. **W. Wang:** Investigation, writing–original draft. **Z. Chen:** Data curation, investigation, writing–review and editing. **H. Xiao:** Data curation, writing–original draft, writing–review and editing. **Q. Zhou:** Data curation, formal analysis, writing–review and editing. **B. Li:** Data curation, formal analysis, writing–review and editing. **Y. Xie:** Data curation, formal analysis, writing–review and editing. **H. Hu:** Data curation, formal analysis, writing–review and editing. **M. He:** Data curation, formal analysis, writing–review and editing. **Y. Han:** Data curation, methodology, writing–review and editing. **L. Tang:** Data curation, writing–review and editing. **Y. Ma:** Data curation, writing–review and editing. **X. Li:** Data curation, writing–review and editing. **X. Zhou:** Data curation, writing–review and editing. **Z. Dai:** Data curation, writing–review and editing. **Z. Liu:** Data curation, writing–review and editing. **J. Tan:** Data curation, writing–review and editing. **L. Xu:** Conceptualization, data curation, writing–review and editing. **S. Li:** Resources, writing–review and editing. **S. Shen:** Resources, writing–review and editing. **D. Li:** Resources, writing–review and editing. **J. Lai:** Resources, writing–review and editing. **B. Peng:** Resources, writing–review and editing. **Z. Peng:** Conceptualization, resources, data curation, supervision, writing–original draft, project administration, writing–review and editing. **M. Kuang:** Conceptualization, resources, data curation, supervision, funding acquisition, investigation, writing–original draft, writing–review and editing.

Acknowledgments

We thank the patients and their families, as well as the investigators and personnel for their significant contribution. Research reported in this publication was supported by the National Science Fund for Distinguished Young Scholars (grant no. 81825013), the National Natural Science Foundation of China (grant nos. 82172047, 81771958, 81770608), the "Ten thousand Talents Program" National Special Support Program for High-level Talents and the National Special Support Plan and the Science and Technology Program of Guangzhou, China (grant no. 201704020215), the Natural Science Foundation of Guangdong Province (grant no. 2021A1515010450), and the Kelin Outstanding Young Scientist of the First Affiliated Hospital, Sun Yat-sen University (grant no. R08030).

The costs of publication of this article were defrayed in part by the payment of page charges. This article must therefore be hereby marked *advertisement* in accordance with 18 U.S.C. Section 1734 solely to indicate this fact.

Received October 31, 2021; revised February 4, 2022; accepted April 27, 2022; published first April 27, 2022.

References

1. EASL. EASL Clinical Practice Guidelines: management of hepatocellular carcinoma. J Hepatol 2018;69:182–236.
2. Villanueva A. Hepatocellular carcinoma. N Engl J Med 2019;380:1450–62.
3. Wang Z, Ren Z, Chen Y, Hu J, Yang G, Yu L, et al. Adjuvant transarterial chemoembolization for HBV-related hepatocellular carcinoma after resection: A Randomized Controlled Study. Clin Cancer Res 2018;24:2074–81.
4. Kohno H, Nagasue N, Hayashi T, Yamanoi A, Uchida M, Ono T, et al. Postoperative adjuvant chemotherapy after radical hepatic resection for hepatocellular carcinoma (HCC). Hepatogastroenterology 1996;43:1405–9.
5. Chen X, Zhang B, Yin X, Ren ZG, Qiu SJ, Zhou J. Lipiodolized transarterial chemoembolization in hepatocellular carcinoma patients after curative resection. J Cancer Res Clin Oncol 2013;139:773–81.
6. Bruix J, Takayama T, Mazzaferro V, Chau GY, Yang JM, Kudo M, et al. Adjuvant sorafenib for hepatocellular carcinoma after resection or ablation (STORM): a phase 3, randomised, double-blind, placebo-controlled trial. Lancet Oncol 2015;16:1344–54.
7. Pinyol R, Montal R, Bassaganyas L, Sia D, Takayama T, Chau GY, et al. Molecular predictors of prevention of recurrence in HCC with sorafenib as adjuvant treatment and prognostic factors in the phase 3 STORM trial. Gut 2019;68:1065–75.
8. Xu LX, He MH, Dai ZH, Yu J, Wang JG, Li XC, et al. Genomic and transcriptional heterogeneity of multifocal hepatocellular carcinoma. Ann Oncol 2019;30:990–7.
9. Ribas A, Wolchok JD. Cancer immunotherapy using checkpoint blockade. Science 2018;359:1350–5.
10. Ribas A, Hamid O, Daud A, Hodi FS, Wolchok JD, Kefford R, et al. Association of pembrolizumab with tumor response and survival among patients with advanced melanoma. JAMA 2016;315:1600–9.
11. Garon EB, Rizvi NA, Hui R, Leighl N, Balmanoukian AS, Eder JP, et al. Pembrolizumab for the treatment of non-small-cell lung cancer. N Engl J Med 2015;372:2018–28.
12. Topalian SL, Hodi FS, Brahmer JR, Gettinger SN, Smith DC, McDermott DF, et al. Safety, activity, and immune correlates of anti-PD-1 antibody in cancer. N Engl J Med 2012;366:2443–54.
13. Zhu AX, Finn RS, Edeline J, Cattan S, Ogasawara S, Palmer D, et al. Pembrolizumab in patients with advanced hepatocellular carcinoma previously treated with sorafenib (KEYNOTE-224): a non-randomised, open-label phase 2 trial. Lancet Oncol 2018;19:940–52.
14. Hu Z, Ott PA, Wu CJ. Towards personalized, tumour-specific, therapeutic vaccines for cancer. Nature Rev Immunol 2018;18:168–82.
15. Schumacher TN, Schreiber RD. Neoantigens in cancer immunotherapy. Science 2015;348:69–74.
16. Coulie PG, Van den Eynde BJ, van der Bruggen P, Boon T. Tumour antigens recognized by T lymphocytes: at the core of cancer immunotherapy. Nat Rev Cancer 2014;14:135–46.
17. Lee JH, Lee JH, Lim YS, Yeon JE, Song TJ, Yu SJ, et al. Adjuvant immunotherapy with autologous cytokine-induced killer cells for hepatocellular carcinoma. Gastroenterology 2015;148:1383–91.
18. Takayama T, Sekine T, Makuuchi M, Yamasaki S, Kosuge T, Yamamoto J, et al. Adoptive immunotherapy to lower postsurgical recurrence rates of hepatocellular carcinoma: a randomised trial. Lancet 2000;356:802–7.
19. Morgan RA, Chinnasamy N, Abate-daga D, Gros A, Robbins PF, Zheng ZL, et al. Cancer regression and neurological toxicity following anti-MAGE-A3 TCR gene therapy. J Immunother 2013;36:133–51.
20. Sahin U, Derhovanessian E, Miller M, Kloke BP, Simon P, Lower M, et al. Personalized RNA mutanome vaccines mobilize poly-specific therapeutic immunity against cancer. Nature 2017;547:222–6.
21. Carreno BM, Magrini V, Becker-hapak M, Kaabinejadian S, Hundal J, Petti AA, et al. Cancer immunotherapy. A dendritic cell vaccine increases the breadth and diversity of melanoma neoantigen-specific T cells. Science 2015;348:803–8.
22. Keskin DB, Anandappa AJ, Sun J, Tirosh I, Mathewson ND, Li SQ, et al. Neoantigen vaccine generates intratumoral T cell responses in phase Ib glioblastoma trial. Nature 2019;565:234–9.
23. Ott PA, Hu Z, Keskin DB, Shukla SA, Sun J, Bozym DJ, et al. An immunogenic personal neoantigen vaccine for patients with melanoma. Nature 2017;547:217–21.
24. Hilf N, Kuttruff-coqui S, Frenzel K, Bukur V, Stevanovic S, Gouttefangeas C, et al. Actively personalized vaccination trial for newly diagnosed glioblastoma. Nature 2019;565:240–5.
25. Leisegang M, Engels B, Schreiber K, Yew PY, Kiyotani K, Idel C, et al. Eradication of large solid tumors by gene therapy with a T-cell receptor targeting a single Cancer-specific point mutation. Clin Cancer Res 2016;22:2734–43.
26. Yamamoto TN, Kishton RJ, Restifo NP. Developing neoantigen-targeted T cell-based treatments for solid tumors. Nat Med 2019;25:1488–99.
27. Lee JH, Lee Y, Lee M, Heo MK, Song JS, Kim KH, et al. A phase I/IIa study of adjuvant immunotherapy with tumour antigen-pulsed dendritic cells in patients with hepatocellular carcinoma. Br J Cancer 2015;113:1666–76.
28. Mangani D, Weller M, Roth P. The network of immunosuppressive pathways in glioblastoma. Biochem Pharmacol 2017;130:1–9.
29. Cucchetti A, Zhong JH, Berhane S, Toyoda H, Shi KQ, Tada T et al. The chances of hepatic resection curing hepatocellular carcinoma. J Hepatol 2020;72:711–7.
30. Hoof I, Peters B, Sidney J, Pedersen LE, Sette A, Lund O, et al. NetMHCpan, a method for MHC class I binding prediction beyond humans. Immunogenetics 2009;61:1–13.
31. Andreatta M, Nielsen M. Gapped sequence alignment using artificial neural networks: application to the MHC class I system. Bioinformatics 2016;32:511–7.
32. Jørgensen KW, Rasmussen M, Buus S, Nielsen M. NetMHCstab - predicting stability of peptide-MHC-I complexes; impacts for cytotoxic T lymphocyte epitope discovery. Immunology 2014;141:18–26.
33. Harndahl M, Rasmussen M, Roder G, Dalgaardpedersen I, Sørensen M, Nielsen M, et al. Peptide-MHC class I stability is a better predictor than peptide affinity of CTL immunogenicity. Eur J Immunol 2012;42:1405–16.
34. Altschul SF, Gish W, Miller W, Myers EW, Lipman DJ. Basic local alignment search tool. J Mol Biol 1990;215:403–10.
35. Robinson JT, Thorvaldsdottir H, Winckler W, Guttman M, Lander ES, Getz G, et al. Integrative genomics viewer. Nat Biotechnol 2011;29:24–6.
36. Li H, Durbin R. Fast and accurate short read alignment with Burrows-Wheeler transform. Bioinformatics 2009;25:1754–60.
37. Mckenna A, Hanna M, Banks E, Sivachenko A, Cibulskis K, Kernytsky A, et al. The Genome Analysis Toolkit: a MapReduce framework for analyzing next-generation DNA sequencing data. Genome Res 2010;20:1297–303.
38. Cibulskis K, Lawrence MS, Carter SL, Sivachenko A, Jaffe D, Sougnez C, et al. Sensitive detection of somatic point mutations in impure and heterogeneous cancer samples. Nat Biotechnol 2013;31:213–9.
39. Wang K, Li M, Hakonarson H. ANNOVAR: functional annotation of genetic variants from high-throughput sequencing data. Nucleic Acids Res 2010;38:e164.
40. Shen R, Seshan VE. FACETS: allele-specific copy number and clonal heterogeneity analysis tool for high-throughput DNA sequencing. Nucleic Acids Res 2016;44:e131.
41. Roth A, Khattra J, Yap D, Wan A, Laks E, Biele J, et al. PyClone: statistical inference of clonal population structure in cancer. Nat Methods 2014;11:396–8.
42. Wang L, Wang S, Li W. RSeQC: quality control of RNA-seq experiments. Bioinformatics 2012;28:2184–5.
43. Zhang Q, Lou Y, Yang J, Wang J, Feng J, Zhao Y, et al. Integrated multiomic analysis reveals comprehensive tumour heterogeneity and novel immunophenotypic classification in hepatocellular carcinomas. Gut 2019;68:2019–31.
44. Ayers M, Lunceford J, Nebozhyn M, Murphy E, Loboda A, Kaufman DR, et al. IFN-γ-related mRNA profile predicts clinical response to PD-1 blockade. J Clin Invest 2017;127:2930–40.
45. Cancer Genome Altas Research Network. Comprehensive and integrative genomic characterization of hepatocellular carcinoma. Cell 2017;169:1327–41.e23.
46. Shukla SA, Rooney MS, Rajasagi M, Tiao G, Dixon PM, Lawrence MS, et al. Comprehensive analysis of cancer-associated somatic mutations in class I HLA genes. Nat Biotechnol 2015;33:1152–8.
47. Mcgranahan N, Rosenthal R, Hiley CT, Rowan AJ, Watkins TBK, Wilson GA, et al. Allele-specific HLA loss and immune escape in lung cancer evolution. Cell 2017;171:1259–71.
48. Rooney MS, Shukla SA, Wu CJ, Getz G, Hacohen N. Molecular and genetic properties of tumors associated with local immune cytolytic activity. Cell 2015;160:48–61.
49. Johnson DB, Frampton GM, Rioth MJ, Yusko E, Xu Y, Guo X, et al. Targeted next generation sequencing identifies markers of response to PD-1 blockade. Cancer Immunol Res 2016;4:959–67.
50. Tate JG, Bamford S, Jubb HC, Sondka Z, Beare DM, Bindal N, et al. COSMIC: the catalogue of somatic mutations in cancer. Nucleic Acids Res 2019;47:D941–7.

51. Han Y, Wu Y, Yang C, Huang J, Guo Y, Liu L, et al. Dynamic and specific immune responses against multiple tumor antigens were elicited in patients with hepatocellular carcinoma after cell-based immunotherapy. J Transl Med 2017;15:64.
52. He Y, Guo Y, Chen J, Hu X, Li X, Kong Y, et al. Multiple antigen stimulating cellular therapy (MASCT) for hepatocellular carcinoma after curative treatment: A retrospective study. J Cancer 2018;9:1385–93.
53. Angelova M, Mlecnik B, Vasaturo A, Bindea G, Fredriksen T, Lafontaine L, et al. Evolution of metastases in space and time under immune selection. Cell 2018; 175:751–65.
54. Tumeh PC, Harview CL, Yearley JH, Shintaku IP, Taylor EJ, Robert L, et al. PD-1 blockade induces responses by inhibiting adaptive immune resistance. Nature 2014;515:568–71.
55. Cancer Genome Atlas Research Network. Comprehensive and integrative genomic characterization of hepatocellular carcinoma. Cell 2017;169: 1327–41.
56. Mascaux C, Angelova M, Vasaturo A, Beane J, Hijazi K, Anthoine G, et al. Immune evasion before tumour invasion in early lung squamous carcinogenesis. Nature 2019;571:570–5.
57. Rosenthal R, Cadieux EL, Salgado R, Bakir MA, Moore DA, Hiley CT, et al. Neoantigen-directed immune escape in lung cancer evolution. Nature 2019;567: 479–85.
58. Corbière V, Chapiro J, Stroobant V, Ma WB, Lurquin C, Lethe B, et al. Antigen spreading contributes to MAGE vaccination-induced regression of melanoma metastases. Cancer Res 2011;71:1253–62.
59. Ott PA, Lieskovan SH, Chmielowski B, Govindan R, Naing A, Bhardwaj N, et al. A phase Ib trial of personalized neoantigen therapy plus anti-PD-1 in patients with advanced melanoma, non-small cell lung cancer, or bladder cancer. Cell 2020;183:347–62.
60. Nduom EK, Weller M, Heimberger AB. Immunosuppressive mechanisms in glioblastoma. Neuro-oncol 2015:i9–14.
61. Ng KKC, Chok KSH, Chan ACY, Cheung TT, Wong TCL, Fung JYY, et al. Randomized clinical trial of hepatic resection versus radiofrequency ablation for early-stage hepatocellular carcinoma. Br J Surg 2017;104:1775–84.
62. Feng K, Yan J, Li XW, Xia F, Ma KS, Wang SG, et al. A randomized controlled trial of radiofrequency ablation and surgical resection in the treatment of small hepatocellular carcinoma. J Hepatol 2012;57:794–802.
63. Chen MS, Li JQ, Zheng Y, Guo RP, Liang HH, Zhang YQ, et al. A prospective randomized trial comparing percutaneous local ablative therapy and partial hepatectomy for small hepatocellular carcinoma. Ann Surg 2006;243:321–8.
64. Kang TW, Kim JM, Rhim HC, Lee MW, Kim YS, Lim HK, et al. Small hepatocellular carcinoma: radiofrequency ablation versus nonanatomic resection-propensity score analyses of long-term outcomes. Radiology 2015; 275:908–19.